THE ASTROPHYSICAL JOURNAL, 196:503–513, 1975 March 1

THE BALMER DISCONTINUITIES OF O9–B2 SUPERGIANTS

R. E. SCHILD AND F. H. CHAFFEE
Center for Astrophysics, Harvard College Observatory and Smithsonian Astrophysical Observatory
Received 1974 July 19; revised 1974 September 9

ABSTRACT

New energy distributions of supergiants at 50 Å resolution from λλ3200–8000 show that the Balmer discontinuities are poorly correlated with spectral types. A particularly good example is ε Ori, whose Balmer discontinuity is 0.1 mag larger than other O9.5 Ia and B0.5 Ia supergiants. Analysis of available four-color and Hβ photometry shows that whereas Hβ correlates well with luminosity as indicated by MK luminosity class, the Balmer discontinuity does not.

Our energy distributions show that several O9.5–B0.5 Ia supergiants have Balmer discontinuities in emission on the Palomar system of absolute calibration. They appear to be continuous across the Balmer discontinuity on the calibration of Hayes.

Subject headings: atmospheres, stellar — early-type stars — luminous stars — spectrophotometry

I. INTRODUCTION

The hot supergiants are among the most poorly understood stars with respect to our knowledge of masses, effective temperatures, dimensions, and atmospheric surface effects. The reasons for this fact are well known: Most supergiants are very distant and reddened and are blowing off their atmospheres at high supersonic velocities. Thus, our ability to measure their intrinsic energy distributions or to compute stellar models for them is severely hampered.

We present observations of OB supergiants made in conjunction with a program for the synthesis of energy distributions of young clusters. In the course of dereddening the fluxes, we have found that the energy distributions are of sufficient intrinsic interest to be worthy of separate discussion.

II. OBSERVATIONS

Energy distributions of the OB supergiant standards of the MK system were measured with the Latham grating spectrometer on the Mount Hopkins 60-inch (1.5 m) Tillinghast reflector. A 50 Å bandpass was used throughout, and the blue and red portions of the spectra were measured on separate nights. Nightly extinction coefficients were computed and applied to our data. The data are reported on the absolute calibration system of Oke and Schild (1970) and are believed to be accurate to ± 0.02 mag at all wavelengths except 8000 Å.

All energy distributions have been corrected for interstellar extinction by the use of the interstellar reddening law of Radick (1973) and Hayes *et al.* (1973). Because Hayes *et al.* and Radick based their results on Whiteoak's (1966) data, which extend only to λ3448, we have had to extend the reddening law for our data to shorter wavelengths with procedures similar to theirs. The observed and corrected fluxes are listed in table 1. We have made no corrections for blocking in our treatment of the data, because such corrections rarely exceed 2 percent for the hot stars and because we make no comparisons with unblanketed models.

III. BALMER DISCONTINUITIES OF THE SUPERGIANTS

In figure 1, we compare our dereddened energy distributions for the O9.5 Ia supergiants α Cam and HD 195592 to the blanketed model atmospheres (25,000, 3.5) of Kurucz, Peytremann, and Avrett (1974). Comparison with a lower surface-gravity model would be preferable, but such models do not exist, owing to the well-known radiation-pressure problem. Here, we do not propose to determine the effective temperatures and gravity of the supergiants; rather, we wish only to show that the Balmer discontinuity appears in *emission* in the two O9.5 Ia supergiants. This is made clear in figure 1 by the dashed line, a smooth extrapolation of the continuum for $\lambda > 4000$ Å with the same slope as the Balmer continuum of the model.

We caution that the appearance of a Balmer discontinuity in emission may be, at least in part, an artifact of the absolute calibration, which still must be considered uncertain across the Balmer discontinuity. Adoption of the calibration of Hayes (1970) gives energy distributions that are continuous across the Balmer jump. Recent calculations by Mihalas and Hummer (1974) of non-LTE spherically extended static atmospheres for $T_{\rm eff} \approx 39{,}500°$ K and $\log g = 3.5$, with a variety of treatments to account for radiation pressure, all show a Balmer jump in absorption. While our stars are presumably cooler than the Mihalas and Hummer (1974) models, they are similarly far from LTE and we would expect to find Balmer jumps in absorption. It is of course well known that supergiants have expanding atmospheres and that the region below the Balmer discontinuity is formed in a relatively high atmospheric layer. These facts suggest that the atmospheric expansion affects the atmospheric structure and continuum formation, and we eagerly await the development of models that incorporate expansion.

TABLE 1

		HD 1383		HD 14143		HD 30614		HD 43818	
λ	1/λ	Observed	Dereddened	Observed	Dereddened	Observed	Dereddened	Observed	Dereddened
3200	3.13	0.34	-0.37	0.70	-0.26	-0.10	-0.44	0.26	-0.50
3250	3.08	0.31	-0.38	0.65	-0.28	-0.11	-0.44	0.22	-0.52
3300	3.03	0.21	-0.43	0.58	-0.29	-0.14	-0.45	0.17	-0.52
3350	2.99	0.25	-0.35	0.55	-0.27	-0.11	-0.40	0.18	-0.47
3400	2.94	0.18	-0.39	0.51	-0.26	-0.14	-0.41	0.15	-0.46
3450	2.90	0.16	-0.37	0.47	-0.25	-0.14	-0.40	0.12	-0.45
3500	2.86	0.15	-0.36	0.45	-0.24	-0.13	-0.37	0.13	-0.42
3571	2.80	0.18	-0.28	0.43	-0.19	-0.09	-0.31	0.14	-0.35
3636	2.75	0.16	-0.26	0.40	-0.17	-0.08	-0.28	0.13	-0.32
4036	2.48	0.05	-0.17	0.15	-0.14	-0.04	-0.14	0.05	-0.18
4167	2.40	0.04	-0.09	0.10	-0.08	-0.02	-0.08	0.04	-0.10
4255	2.35	0.03	-0.08	0.08	-0.07	-0.01	-0.06	0.03	-0.09
4464	2.24	0.00	0.00	0.00	0.00	0.00	0.00	0.00	0.00
4566	2.19	0.00	0.04	-0.01	0.04	0.02	0.04	-0.01	0.03
4780	2.09	-0.02	0.10	-0.09	0.07	0.07	0.13	-0.03	0.10
5000	2.00	-0.04	0.20	-0.15	0.17	0.09	0.20	-0.05	0.21
5263	1.90	-0.11	0.27	-0.29	0.22	0.12	0.30	-0.10	0.31
5556	1.80	-0.14	0.36	-0.37	0.31	0.14	0.38	-0.12	0.42
5840	1.71	-0.12	0.47	-0.41	0.39	0.18	0.46	-0.13	0.50
6050	1.65	-0.11	0.53	-0.43	0.44	0.21	0.52	-0.13	0.56
6430	1.56	-0.09	0.65	-0.46	0.54	0.27	0.63	-0.12	0.67
6821	1.47	-0.10	0.74	-0.51	0.63	0.31	0.72	-0.14	0.76
7102	1.41	-0.10	0.80	-0.54	0.68	0.36	0.79	-0.14	0.83
7530	1.33	-0.09	0.90	-0.59	0.75	0.40	0.88	-0.13	0.93
7780	1.29	-0.11	0.93	-0.57	0.83	0.41	0.91	-0.14	0.97
8060	1.24	-0.09	0.99	-0.60	0.86	0.45	0.97	-0.13	1.03

TABLE 1—*Continued*

λ	1/λ	HD 190919		HD 192422		HD 194839		HD 195592	
		Observed	Dereddened	Observed	Dereddened	Observed	Dereddened	Observed	Dereddened
3200	3.13	0.31	-0.28	0.69	-0.40	1.28	-0.41	1.10	-0.41
3250	3.08	0.28	-0.29	0.63	-0.42	1.20	-0.44	1.01	-0.45
3300	3.03	0.24	-0.30	0.57	-0.42	1.10	-0.44	0.92	-0.45
3350	2.99	0.24	-0.26	0.55	-0.38	1.05	-0.39	0.88	-0.41
3400	2.94	0.21	-0.26	0.48	-0.39	0.97	-0.38	0.80	-0.41
3450	2.90	0.18	-0.27	0.45	-0.37	0.90	-0.38	0.74	-0.40
3500	2.86	0.19	-0.23	0.43	-0.35	0.86	-0.35	0.70	-0.38
3571	2.80	0.20	-0.18	0.42	-0.29	0.81	-0.29	0.66	-0.32
3636	2.75	0.19	-0.16	0.39	-0.26	0.75	-0.26	0.61	-0.29
4036	2.48	0.04	-0.14	0.15	-0.18	0.35	-0.17	0.30	-0.16
4167	2.40	0.03	-0.08	0.10	-0.11	0.24	-0.08	0.21	-0.08
4255	2.35	0.01	-0.08	0.06	-0.11	0.17	-0.10	0.15	-0.09
4464	2.24	0.00	0.00	0.00	0.00	0.00	0.00	0.00	0.00
4566	2.19	-0.01	0.02	-0.02	0.04	-0.06	0.03	-0.06	0.02
4780	2.09	-0.05	0.05	-0.09	0.09	-0.24	0.04	-0.20	0.05
5000	2.00	-0.06	0.14	-0.14	0.23	-0.40	0.17	-0.36	0.15
5263	1.90	-0.10	0.21	-0.27	0.31	-0.65	0.25	-0.56	0.24
5556	1.80	-0.12	0.30	-0.38	0.39	-0.85	0.35	-0.75	0.32
5840	1.71	-0.10	0.39	-0.43	0.47	-1.00	0.41	-0.88	0.37
6050	1.65	-0.09	0.45	-0.45	0.54	-1.08	0.46	-0.95	0.42
6430	1.56	-0.07	0.55	-0.00	–	-1.21	0.56	-1.06	0.52
6821	1.47	-0.08	0.62	-0.51	0.78	-1.40	0.61	-1.23	0.56
7102	1.41	-0.08	0.67	-0.54	0.85	-1.47	0.68	-1.27	0.65
7530	1.33	-0.05	0.77	-0.55	0.97	-1.55	0.81	-1.37	0.73
7780	1.29	-0.04	0.82	-0.58	1.01	-1.61	0.87	-1.41	0.80
8060	1.24	-0.04	0.86	-0.60	1.06	-1.70	0.88	-1.49	0.81

TABLE 1—*Continued*

λ	1/λ	HD 199216		HD 204172		HD 209975		HD 216411	
		Observed	Dereddened	Observed	Dereddened	Observed	Dereddened	Observed	Dereddened
3200	3.13	0.70	-0.35	-0.17	-0.43	0.04	-0.42	0.79	-0.32
3250	3.08	0.62	-0.40	-0.18	-0.43	0.01	-0.43	0.72	-0.36
3300	3.03	0.55	-0.40	-0.20	-0.44	-0.04	-0.46	0.62	-0.39
3350	2.99	0.52	-0.38	-0.18	-0.40	-0.01	-0.40	0.63	-0.32
3400	2.94	0.47	-0.37	-0.19	-0.40	-0.04	-0.41	0.51	-0.38
3450	2.90	0.44	-0.35	-0.18	-0.38	-0.05	-0.40	0.48	-0.36
3500	2.86	0.42	-0.33	-0.16	-0.35	-0.03	-0.36	0.46	-0.34
3571	2.80	0.36	-0.32	-0.13	-0.30	0.00	-0.30	0.43	-0.29
3636	2.75	0.36	-0.26	-0.11	-0.27	0.00	-0.27	0.40	-0.26
4036	2.48	0.10	-0.22	-0.08	-0.16	-0.01	-0.15	0.21	-0.13
4167	2.40	0.06	-0.14	-0.04	-0.09	0.00	-0.09	0.13	-0.08
4255	2.35	0.04	-0.13	-0.03	-0.07	0.00	-0.07	0.09	-0.09
4464	2.24	0.00	0.00	0.00	0.00	0.00	0.00	0.00	0.00
4566	2.19	-0.03	0.03	0.03	0.04	0.01	0.03	-0.02	0.04
4780	2.09	-0.11	0.07	0.07	0.11	0.03	0.11	-0.14	0.05
5000	2.00	-0.17	0.18	0.12	0.21	0.04	0.19	-0.23	0.14
5263	1.90	-0.32	0.24	0.17	0.31	0.04	0.28	-0.37	0.22
5556	1.80	-0.39	0.35	0.21	0.40	0.05	0.38	-0.48	0.31
5840	1.71	-0.41	0.46	0.28	0.50	0.09	0.47	-0.53	0.40
6050	1.65	-0.47	0.48	0.32	0.56	0.12	0.54	-0.57	0.44
6430	1.56	-0.52	0.58	0.39	0.66	0.17	0.65	-0.63	0.53
6821	1.47	-0.54	0.71	0.44	0.75	0.18	0.73	-0.69	0.64
7102	1.41	-0.51	0.83	0.50	0.83	0.21	0.79	-0.75	0.67
7530	1.33	-0.54	0.92	0.58	0.95	0.27	0.91	-0.78	0.78
7780	1.29	-0.56	0.98	0.59	0.97	0.27	0.94	-0.80	0.83
8060	1.24	-0.56	1.04	0.66	1.06	0.32	1.02	-0.83	0.87

TABLE 1—*Continued*

		NGC 581 #3*		NGC 6913 #2		NGC 6913 #3		NGC 6913 #4	
λ	1/λ	Observed	Dereddened	Observed	Dereddened	Observed	Dereddened	Observed	Dereddened
3200	3.13	0.44	-0.25	1.23	-0.40	1.38	-0.33	1.11	-0.46
3250	3.08	0.42	-0.21	1.15	-0.33	1.27	-0.29	1.04	-0.38
3300	3.03	0.37	-0.20	1.05	-0.30	1.17	-0.26	0.92	-0.38
3350	2.99	0.37	-0.17	0.98	-0.32	1.10	-0.27	0.89	-0.35
3400	2.94	0.34	-0.17	0.92	-0.30	1.03	-0.25	0.82	-0.34
3450	2.90	0.33	-0.14	0.87	-0.29	0.95	-0.26	0.77	-0.33
3500	2.86	0.33	-0.11	0.81	-0.29	0.89	-0.25	0.72	-0.32
3571	2.80	0.35	-0.06	0.78	-0.21	0.83	-0.23	0.68	-0.29
3636	2.75	0.33	-0.05	0.70	-0.23	0.80	-0.17	0.63	-0.26
4036	2.48	0.02	-0.17	0.31	-0.16	0.33	-0.16	0.28	-0.16
4167	2.40	0.04	-0.10	0.20	-0.12	0.21	-0.11	0.18	-0.13
4255	2.35	0.01	-0.08	0.15	-0.06	0.16	-0.06	0.12	-0.09
4464	2.24	0.00	0.00	0.00	0.00	0.00	0.00	0.00	0.00
4566	2.19	0.00	0.05	-0.05	0.05	-0.04	0.08	-0.06	0.03
4780	2.09	-0.04	0.08	-0.18	0.10	-0.23	0.06	-0.19	0.08
5000	2.00	-0.05	0.15	-0.32	0.15	-0.37	0.13	-0.31	0.13
5263	1.90	-0.10	0.27	-0.54	0.30	-0.55	0.34	-0.50	0.31
5556	1.80	-0.14	0.32	-0.71	0.34	-0.73	0.38	-0.66	0.35
5840	1.71	-0.10	0.42	-0.79	0.40	-0.85	0.41	-0.74	0.41
6050	1.65	-0.09	0.50	-0.90	0.45	-0.92	0.52	-0.79	0.53
6430	1.56	-0.07	0.61	-0.94	0.64	-1.00	0.66	-0.86	0.67
6821	1.47	-0.06	0.72	-1.02	0.78	-1.12	0.77	-0.96	0.76
7102	1.41	-0.07	0.77	-1.10	0.84	-1.20	0.84	-1.01	0.85
7530	1.33	-0.05	0.86	-1.15	0.95	-1.27	0.94	-1.06	0.95
7780	1.29	-0.04	1.01	-1.20	1.00	-1.31	1.02	-1.09	1.03
8060	1.24	-0.08	1.09	-1.26	1.04	-1.38	1.06	-1.15	1.06

*Numbers are from Hoag et al. (1961).

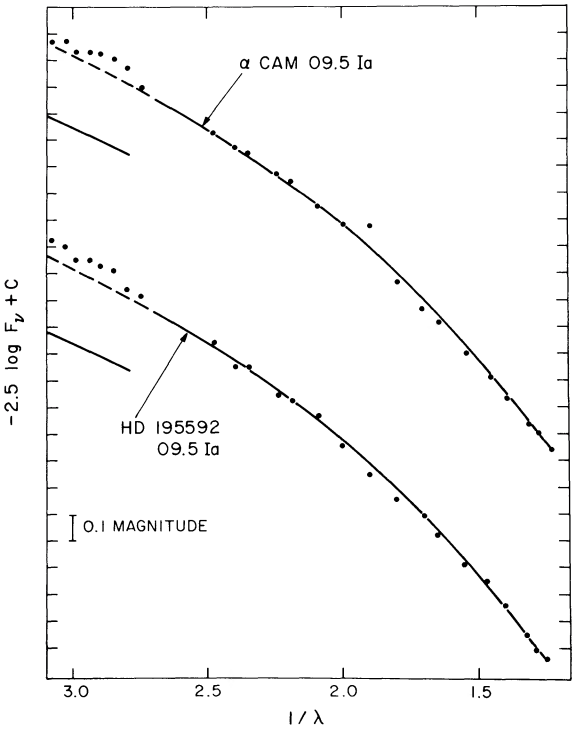

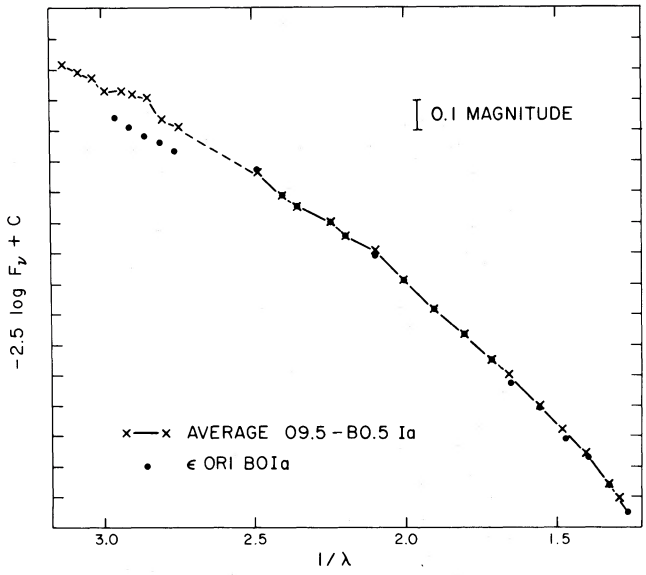

FIG. 1 (*left*).—Energy distribution λλ3200–8000 of two O9.5 Ia supergiants, showing the apparent negative (emission) Balmer discontinuities.

FIG. 2 (*right*).—Energy distribution of ε Ori (B0 Ia) compared with the average for O9.5 Ia–B0.5 Ia stars, showing the significantly more positive Balmer discontinuity.

In figure 2, we compare the energy distribution of ε Ori (B0 Ia) to a mean energy distribution of the three Ia supergiants, α Cam (O9.5 Ia), HD 195592 (O9.5 Ia), and HD 194839 (B0.5 Ia), which have comparable negative Balmer discontinuities and whose average curve is quite smooth. In the Paschen continuum, ε Ori agrees well with the mean curve for the three supergiants; in the Balmer continuum, however, ε Ori is fainter by 0.1 mag. We had expected to find the Balmer discontinuity to increase monotonically with advancing spectral type. We believe ε Ori is a clear exception and but one of several that could be shown to illustrate our general finding that *among the supergiant MK standards, the amounts of the Balmer discontinuities are poorly correlated with spectral type.*

We have chosen to illustrate our point with ε Ori because it is a reasonably certain yet exceptional case. All our Ia supergiants of spectral type B1 and earlier have negative Balmer discontinuities, except for ε Ori, which has a positive discontinuity of 0.06 mag. The data for ε Ori are quite certainly correct: It is one of the original Oke (1964) spectrophotometric standards and has been compared frequently with the others. There is no question of the spectral type of ε Ori, since it has always been a B0 Ia standard and is a fundamental (dagger) standard of the new classifications of Morgan and Keenan (1973). Furthermore, its absolute magnitude is known from its membership in the Ori Ib association; its absolute visual magnitude of −6.8 puts it definitely in the Ia luminosity class.

We list in table 2 the Balmer discontinuities for all the supergiants in table 1, given in order of increasing amount, so as to illustrate further the poor correlation with spectral type. These Balmer discontinuities were estimated by graphically fitting the extrapolated Paschen continuum of Kurucz *et al.*'s (1973) blanketing-corrected models to the dereddened observations of table 1. We used the (25,000, 3.5) model for all stars except the O9.5 and B2 stars, for which we used a (30,000, 3.5) model and a (20,000, 3.0) model, respectively. We have checked the Hayes *et al.* (1973) reddening law with our own data for highly reddened and little reddened supergiants, and we find good agreement. From successive fits to models with somewhat different reddening laws and reddening amounts, we believe that the Balmer discontinuities have been estimated self-consistently to 0.02 mag, although systematic errors, such as an error in the adopted Balmer jump of Vega, could necessitate a uniform revision of the entire scale. We note that adoption of the Hayes (1970) calibration of Vega would make all Balmer jumps 0.05 mag more positive and would thus eliminate the negative Balmer jumps in the Ia supergiants.

Only four of the stars for which we have determined Balmer jumps have previous determinations by Chalonge and Divan (1952). Our Balmer jumps cor-

TABLE 2

Name*	HD	Spectral Type	Balmer Discontinuity
	195592	O9.5 Ia	-0.05
α Cam	30614	O9.5 Ia	-0.04
	194839	B0.5 Ia	-0.02
	216411	B1 Ia	-0.03
	43818	B0 II	+0.02
69 Cyg	204172	B0 Ib	+0.02
19 Cep	209975	O9.5 Ib	+0.03
	1383	B1 II	+0.03
	192422	B0.5 Ib	+0.04
ε Ori	37128	B0 Ia	+0.06
6913 #4†	–	O9.5 III	+0.07
	190919	B1 Ib	+0.06
	14143	B2 Ia	+0.08
6913 #2	–	B0 II	+0.12
	199216	B1 II	+0.13
6913 #3	–	B0 Iab	+0.14
581 #3	–	B2 III	+0.24

*Stars lacking HD numbers are identified by their cluster NGC number, followed by the identifying number.

†Numbers are from Hoag et al. (1961).

relate with theirs and also with $[u - b]$ for three stars. The fourth, 19 Cep, is discrepant in the comparison of all the available photometry. We suggest that the Balmer jump of 19 Cep may have actually changed.

IV. FOUR-COLOR AND Hβ PHOTOMETRY OF SUPERGIANTS

To check our finding that the Balmer jumps are poorly correlated with MK spectral type, we have analyzed the published four-color and Hβ photometry of all luminosity class I and II supergiants of spectral types B2 and earlier. Using data taken from the published surveys of Crawford and associates (Crawford, Barnes, and Golson 1970, 1971*a*, *b*; Crawford, Glaspey, and Perry 1970; Crawford *et al.* 1971), we have derived $(b - y)_0$ and c_0 by conventional procedures. We recall that $(b - y)_0$ measures the slope of the Paschen continuum, whereas for early-type stars, c_0 primarily measures the Balmer jump. The spectral types of the supergiants are generally taken from Morgan, Whitford, and Code (1955) and Hiltner (1956). Stars with Hβ and four-color photometry are listed in table 3.

Figure 3 is a (c_0, Hβ)-diagram for the B1 supergiants; the different luminosity classes are shown separately. We have used spectral type B1 because published data are available for twice as many B1 stars as for other types. We recall that at spectral type B1, classification can be done with good accuracy because the lines of O II and Si III are strong and sensitive to luminosity.

The (c_0, Hβ)-diagram appears to show that the MK luminosity class is well correlated with Hβ but not with c_0. With only two exceptions, the Hβ photometry has completely separated the four luminosity classes and has even separated those of Ia+ from those of Ia. This result is surprising, since hydrogen-line strength is not a primary criterion of luminosity class in MK

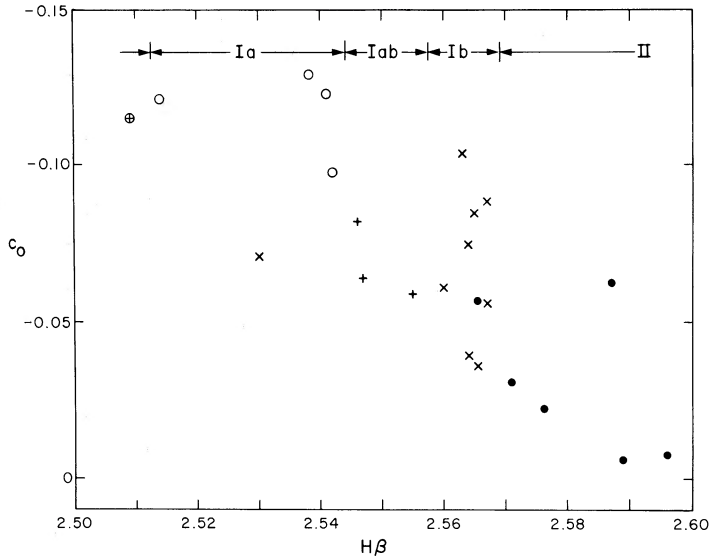

FIG. 3.—The c_0, Hβ diagram for B1 supergiants. Whereas Hβ appears to be well correlated with MK luminosity class, c_0 is evidently not. Symbols denote luminosity class as follows: (●) = II, (×) = Ib, (+) = Iab, (○) = Ia, and (⊕) = Ia+.

TABLE 3

Star HD	Spectral type	Hβ	m_1	c_1	(b - y)	c_0	$(b - y)_0$	[u - b]
290	B1 Ia	2.514	-0.042	-0.059	0.176	-0.121	-0.132	-0.115
13854	B1 Iab	2.546	-0.080	0.008	0.285	-0.082	-0.128	-0.106
14818	B2 Ia	2.526	-0.076	0.050	0.303	-0.035	-0.124	-0.054
24398	B1 Ib	2.564	-0.020	0.015	0.143	-0.039	-0.124	-0.002
30614	O9.5 Ia	2.530	0.014	-0.110	0.080	-0.153	-0.135	-0.069
37128	B0 Ia	2.557	0.026	-0.090	-0.032	-0.110	-0.131	-0.043
38771	B0.5 Ia	2.564	0.026	-0.084	-0.036	-0.103	-0.130	-0.038
40111	B1 Ib	2.565	0.018	-0.053	0.030	-0.085	-0.128	-0.012
41117	B2 Ia	2.513	-0.080	-0.022	0.292	-0.106	-0.131	-0.135
44743	B1 II	2.596	0.052	-0.002	-0.090	-0.008	-0.121	0.088
47432	O9.5 II	2.545	-0.042	-0.084	0.181	-0.147	-0.135	-0.139
52089	B2 II	2.577	0.078	-0.002	-0.081	-0.010	-0.121	0.141
52382	B1 Ib	2.530	-0.050	-0.001	0.222	-0.071	-0.127	-0.065
54764	B1 II	2.587	0.029	-0.016	0.107	-0.063	-0.126	0.059
57061	O9 Ib	2.564	0.054	-0.120	-0.048	-0.137	-0.134	-0.020
64760	B0.5 Ib	2.563	0.042	-0.086	-0.030	-0.106	-0.131	-0.007
68450	O9.5 II	2.556	0.018	-0.087	0.075	-0.129	-0.133	-0.039
86606	B1 Ib	2.567	0.061	-0.063	0.000	-0.089	-0.129	0.059
91316	B1 Iab	2.555	0.033	-0.039	-0.025	-0.059	-0.126	0.023
109867	B1 Ia	2.542	0.015	-0.051	0.104	-0.098	-0.130	-0.004
112244	O9 Ib	2.543	0.029	-0.142	0.079	-0.185	-0.139	-0.071
115842	B0.5 Ia	2.528	-0.037	-0.084	0.296	-0.171	-0.137	-0.111
122879	B0 Ia	2.559	-0.017	-0.088	0.164	-0.148	-0.135	-0.096
141318	B2 II	2.593	0.014	0.122	0.081	0.083	-0.112	0.163
148688	B1 Ia+	2.509	-0.090	-0.019	0.349	-0.115	-0.132	-0.143
149038	B0 Ia	2.551	-0.011	-0.074	0.130	-0.127	-0.133	-0.075
149404	O9 Ia	2.516	-0.010	-0.107	0.331	-0.201	-0.140	-0.074
150168	B1 III	2.565	-0.005	-0.018	0.067	-0.057	-0.126	-0.017
150898	B0.5 Ia	2.554	0.025	-0.100	0.019	-0.130	-0.133	-0.047
152003	O9.5 Ib	2.554	-0.093	-0.052	0.371	-0.152	-0.135	-0.179
152147	O9.5 Ib	2.562	-0.062	-0.071	0.371	-0.171	-0.137	-0.136
152234	B0.5 Ia	2.551	-0.033	-0.066	0.226	-0.138	-0.134	-0.096
152235	B1 Ia	2.541	-0.106	-0.003	0.468	-0.123	-0.132	-0.140
152236	B1.5 Iap+	2.499	-0.102	-0.049	0.440	-0.163	-0.136	-0.183
152249	O9.5 Ib	2.554	-0.016	-0.099	0.215	-0.169	-0.137	-0.097
152405	O9.5 Ib	2.566	-0.025	-0.089	0.178	-0.151	-0.135	-0.111

TABLE 3—*Continued*

Star HD	Spectral type	Hβ	m_1	c_1	(b - y)	c_0	$(b - y)_0$	[u - b]
152424	O9 Ia	2.547	-0.064	-0.068	0.369	-0.168	-0.137	-0.137
152667	B0.5 Ia	2.521	-0.060	-0.088	0.273	-0.170	-0.137	-0.164
154090	B1 Ia	2.538	-0.046	-0.010	0.265	-0.089	-0.129	-0.060
154368	O9 Ia	2.549	-0.109	-0.014	0.459	-0.132	-0.133	-0.159
155450	B1 II	2.576	-0.023	0.030	0.135	-0.021	-0.122	0.006
157426	B1 Ib	2.560	0.034	-0.040	-0.023	-0.061	-0.126	0.024
164402	B0 Ib	2.585	0.007	-0.070	0.074	-0.111	-0.131	-0.044
164637	B0 II	2.592	0.020	-0.067	0.056	-0.104	-0.130	-0.018
165024	B2 Ib	2.583	0.035	0.027	0.004	0.002	-0.120	0.098
165516	B0.5 Ib	2.575	0.010	-0.046	0.145	-0.101	-0.130	-0.003
165793	B1 II	2.571	0.011	0.004	0.054	-0.031	-0.123	0.035
167263	O9 II	2.578	-0.001	-0.086	0.089	-0.130	-0.133	-0.074
167264	B0 Ia	2.562	0.102	0.003	-0.080	-0.005	-0.121	0.194
167756	B0.5 Ia	2.554	0.021	-0.083	-0.015	-0.106	-0.131	-0.043
168021	B0 Ib	2.575	-0.055	-0.032	0.276	-0.113	-0.131	-0.098
185859	B0.5 Ia	2.562	-0.074	-0.059	0.343	-0.155	-0.135	-0.152
188209	O9.5 Ia	2.552	0.032	-0.102	0.006	-0.130	-0.133	-0.037
190603	B1.5 Ia	2.492	-0.105	0.009	0.470	-0.111	-0.131	-0.126
191877	B1 Ib	2.566	0.000	0.004	0.076	-0.036	-0.124	0.016
204172	B0 Ib	2.544	0.010	-0.077	0.016	-0.106	-0.131	-0.054
205139	B1 Ib	2.567	-0.028	0.004	0.175	-0.056	-0.126	-0.024
206165	B2 Ib	2.560	-0.051	0.135	0.275	0.057	-0.114	0.077
207198	O9 II	2.544	-0.016	-0.045	0.281	-0.128	-0.133	-0.032
209975	O9.5 Ib	2.547	-0.002	-0.083	0.127	-0.135	-0.134	-0.067
213087	B0.5 Ib	2.565	-0.081	0.008	0.341	-0.086	-0.129	-0.099
NGC 6871-2	B1 Ib	2.564	-0.02	0.00	0.25	-0.075	-0.128	0.0
NGC 6871-3	B1 Ib	2.563	-0.01	-0.03	0.24	-0.104	-0.130	-0.012
NGC 6871-5	B0 Ib	2.579	-0.02	-0.04	0.26	-0.038	-0.124	-0.038
h+χ Per 003	B2 Ib	2.568	-0.053	0.051	0.244	-0.021	-0.122	-0.016
h+χ Per 16	B1 Iab	2.547	-0.074	0.016	0.280	-0.064	-0.126	-0.087
h+χ Per 612	B1 II	2.589	-0.051	0.070	0.255	-0.006	-0.121	0.009
h+χ Per 1162	B2 Ia	2.546	-0.114	0.101	0.443	-0.012	-0.121	-0.056
h+χ Per 1899	B2 II	2.586	-0.045	0.138	0.289	0.057	-0.114	0.094
h+χ Per 2227	B2 II	2.584	-0.084	0.111	0.328	0.022	-0.118	-0.005
h+χ Per 2541	B2 II	2.610	-0.070	0.146	0.292	0.065	-0.114	0.053

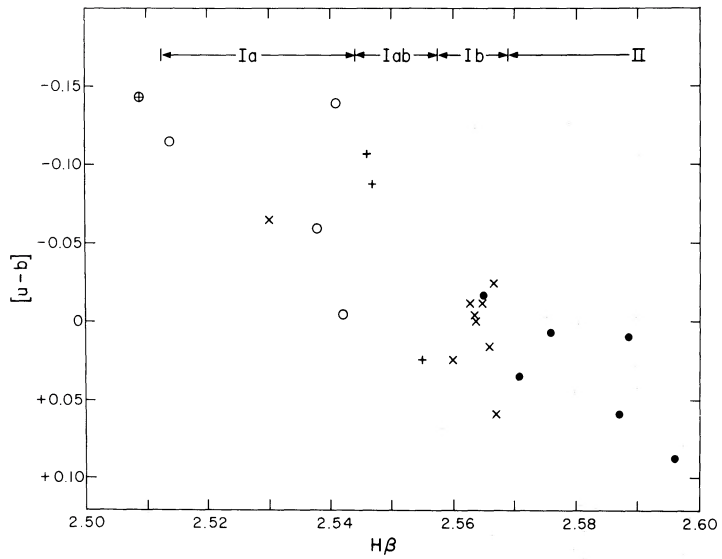

FIG. 4.—The ($[u - b]$, Hβ)-diagram for B1 supergiants. Symbols have the same meaning as in fig. 3. The poor correlation between $[u - b]$ and either Hβ or MK luminosity class is again evident.

classification. On the other hand, we find that the c_0 index is very poorly correlated with luminosity class and shows large variations at a given luminosity class. For example, we see that the B1 Ib stars have 0.07-mag scatter in c_0 and the B1 Iab stars are well within the range of the B1 Ib stars in c_0. We interpret this as confirmation of our finding from continuum energy distributions that the Balmer jumps are poorly correlated with spectral type (including luminosity class).

We note, however, two stars that differ from the Hβ–Sp relation (fig. 3), both of which have been classified by Morgan *et al.* (1955). HD 150168 is a luminosity class II bright giant with Ib Hβ. Its c_0 overlaps with both Ib and II, and the discrepancy is minor. On the other hand, HD 52382 has an Hβ that differs by two subclasses from its Ib luminosity class, also assigned by Morgan *et al.* We suggest that HD 52382 may have Hβ emission, which is common in Ia supergiants (Osmer 1973) but rarely seen in Ib supergiants.

Because c_0 measures not only the Balmer discontinuity but also line blocking in the λ4800 region, we present in figure 4 a ($[u - b]$, Hβ)-diagram for the stars in table 3. We have followed the procedures of Strömgren (1966) and computed $[u - b]$ from the reddening-free indices $[c_1]$ and $[m_1]$ through the relation $[u - b] = [c_1] + 2[m_1]$. The results in figure 4 appear to confirm the conclusion from figure 3—namely, that the Balmer discontinuity in B1 supergiants is poorly correlated with MK luminosity class or Hβ. There is some suggestion that $[u - b]$ shows the greatest variation in the Ia and Iab supergiants, but the number of stars available is too small for such a general statement. We note that the range in $[u - b]$ for Ia and Iab supergiants is almost 0.15 mag; this is slightly greater than the difference in Balmer discontinuities between ϵ Ori and the O9.5–B0.5 Ia supergiants.

V. THE INTRINSIC COLORS OF SUPERGIANTS

The intrinsic colors of the supergiants have not yet been calibrated on the four-color system, probably at least in part because of the problem of the variability of the Balmer jump. With our present empirical understanding of the origin of the problem, we attempt here a calibration of a limited portion of the H-R diagram. This is only a preliminary calibration; we are waiting for an observational program designed for this purpose to be carried out.

Table 4 lists the intrinsic $(b - y)_0$ colors of the O9–B2 supergiants. We note that all the entries for Iab are interpolations, which is not serious, because the luminosity dependence of $(b - y)_0$ is slight. From the agreement at spectral types where data for several

TABLE 4

Spectral Type	$(b-y)_0$					
	O9	O9.5	B0	B0.5	B1	B2
Ia	-0.137	-0.135	-0.133	-0.132	-0.131	-0.126
Iab	-0.136	-0.135	-0.132	-0.131	-0.128	-0.122
Ib	-0.136	-0.135	-0.131	-0.130	-0.126	-0.119
II	-0.135	-0.134	-0.130	-0.127	-0.121	-0.114

TABLE 5

Spectral Type	Hβ
B1 Ia	2.540
B1 Iab	2.552
B1 Ib	2.565
B1 II	2.584

stars are available, we estimate the uncertainty of our means to be 0.003 mag.

We had insufficient data to calibrate Hβ at all spectral types except B1. The scant data available suggested that the Hβ–luminosity-class correlation derived for B1 is applicable at B0 to B2, and the relation is given in table 5.

We thank Dr. C. Payne-Gaposchkin for delightful and stimulating discussions about supergiants and for her comments on the manuscript. We also thank S. Perrenod and J. Mariska for assistance with the reddening corrections and Dr. R. Kurucz for helpful discussions and unpublished blanketed models.

REFERENCES

Chalonge, D., and Divan, L. 1952, *Ann. der Ap.*, **15**, 201.
Crawford, D. L., Barnes, J. V., and Golson, J. C. 1970, *A.J.*, **75**, 624.
———. 1971*a*, *ibid.*, **76**, 621.
———. 1971*b*, *ibid.*, p. 1058.
Crawford, D. L., Barnes, J. V., Hill, G., and Perry, C. L. 1971, *A.J.*, **76**, 1048.
Crawford, D. L., Glaspey, J. W., and Perry, C. L. 1970, *A.J.*, **75**, 822.
Hayes, D. S. 1970, *Ap. J.*, **159**, 165.
Hayes, D. S., Mavko, G. E., Radick, R. R., Rex, K. H., and Greenberg, J. M. 1973, in *IAU Symposium No. 52*, ed. J. M. Greenberg and H. C. van de Hulst (Boston: Reidel), p. 83.
Hiltner, W. A. 1956, *Ap. J. Suppl.*, **2**, 389.
Hoag, A. A., Johnson, H. L., Iriarte, B., Mitchell, R. I., Hallam, K. L., and Sharpless, S. 1961, *Pub. U.S. Naval Obs.*, **17**, 349.
Kurucz, R. L., Peytremann, E., and Avrett, E. H. 1974, *Blanketed Model Atmospheres for Early-Type Stars* (Washington: Smithsonian Institution Press).
Mihalas, D., and Hummer, D. G. 1974, *Ap. J.* (*Letters*), **189**, L39.
Morgan, W. W., and Keenan, P. C. 1973, *Ann. Rev. Astr. and Ap.*, **11**, 29.
Morgan, W. W., Whitford, A. E., and Code, A. D. 1955, *Ap. J. Suppl.*, **2**, 41.
Oke, J. B. 1964, *Ap. J.*, **140**, 689.
Oke, J. B., and Schild, R. E. 1970, *Ap. J.*, **161**, 1015.
Osmer, P. S. 1973, *Ap. J.*, **186**, 459.
Radick, R. 1973, unpublished thesis, Rensselaer Polytechnic Institute.
Strömgren, B. 1966, *Ann. Rev. Astr. and Ap.*, **4**, 433.
Whiteoak, J. 1966, *Ap. J.*, **144**, 305.

RUDOLPH E. SCHILD and FREDERIC H. CHAFFEE: Smithsonian Astrophysical Observatory, 60 Garden Street, Cambridge, Ma 02138